An atomic scale investigation of the adsorption of sodium oleate on Ca²⁺ activated quartz surface

Guichen Gong, Jie Liu, Yuexin Han, Yimin Zhu

College of Resources and Civil Engineering, Northeastern University, Shenyang 110819, China

Corresponding author: liujie@mail.neu.edu.cn (Jie Liu)

Abstract: In this study, the surface properties and flotation behavior of quartz with NaOl as a collector in the presence of Ca^{2+} ions were investigated using density functional theory (DFT) calculations in conjunction with flotation tests, adsorption experiments, zeta potential measurements, and solution chemistry calculations. The results of the flotation and adsorption tests proved that Ca^{2+} promoted the flotation recovery and the adsorption density of sodium oleate on quartz at pH > 8. Zeta potential analyses and solution chemistry calculations demonstrated that $Ca(OH)^+$ was the functional species which activated quartz. DFT calculations indicated that O atoms dominated the quartz (101) surface, and great electrostatic repulsion and space resistance existed between the surface and oleate anion.The spontaneous adsorption of H_2O and OH^- on the (101) surface made quartz surfaces hydrated and hydroxylated, and resulted in the hydrophilicity of quartz. The adsorption of $Ca(OH)^+$ on quartz (101) surface was more favorable and able to repulse the water film, which decreased the electrostatic repulsion and space resistance, and further facilitated the adsorption of oleate anion. During the activating and collecting adsorption processes, electron transition occurred along the $O1-Ca-O2$ path, implying $Ca(OH)^+$ acted as an intermediary and electron donor in the activation process.

Keywords: quartz, sodium oleate, $Ca(OH)^+$, density functional theory

1. Introduction

For having the advantages of good separation efficiency and high economic benefit, the anionic reverse flotation has been the most commonly used way to reduce the quartz content and raise the iron content in hematite concentrations in China (Yin et al., 2016). During this operation, quartz is the desired mineral, and fatty acids are usually used as the collectors (Luo et al., 2016). However, quartz mineral has no flotation behavior in fatty acid collector systems unless it is activated. Many multivalent metal cations can activate quartz in anionic reverse flotation, such as Ca^{2+}, Mg^{2+}, Cu^{2+}, Pb^{2+}, Fe^{3+}, Ba^{2+}, and Al^{3+} (El-salmawy et al., 1993; Fornasiero and Ralston, 2005; Zhang et al., 2014; Jin et al., 2016), and Ca^{2+} is the primarily used one in industry (Ye and Matsuoka, 1993).

In the past decades, the effect of Ca^{2+} in quartz activation has been widely investigated by many researchers using adsorption experiments, atomic force microscope, FTIR spectroscopy, and quartz crystal microbalance, and some theories have been proposed. Guo et al. (2018) summarized that Ca^{2+} can adsorb on the O sites on quartz surfaces, and provides active sites for the following adsorption of fatty acids. Ozkan et al. (2009) and Fuerstenau et al. (2007) concluded that the adsorption of multivalent ion hydroxy complexes increases the adsorption density of anionic collectors on quartz surfaces. Wang (1988) believed that $Ca(OH)_2$ precipitate is the real effective component which activates quartz.

Unfortunately, these concepts were put forward based on ex-site qualitative methods, and no direct evidences were found. The reason for that fatty acids cannot adsorb on quartz is still unknown, and the exact functional activating specie in the solutions is controversial. Therefore, the purpose of this paper was to provide quantitative and in-situ investigation on the activation and flotation mechanisms of quartz using sodium oleate as a collector and Ca^{2+} as an activator. The surface properties of quartz and the adsorption of oleate on activated quartz surface were studied using flotation tests, adsorption

experiments, zeta potential measurements, solution chemistry calculations, and DFT calculations at an atomic scale.

2.   Materials and methods

2.1. Materials

The quartz mineral crystals were obtained from an iron mine in Liaoning province, China. After being manually crushed, ground in a ceramic ball mill and soaked in 5% HCl for 48 h, the samples had a purity of 99.40%, and no other impurity was detected in the XRD measurement. Then, the samples were wet sieved to obtain the -45+25 µm size fraction for the flotation tests and adsorption experiments, the -25 µm size fraction was further ground to finer than 5 µm for the zeta potential measurements.

The collector sodium oleate, the pH regulators NaOH and HCl, and the activator $CaCl_2$ were bought from Tianjin Kemiou Chemical Reagent Co., Ltd., China, which were all of an analytical purity. The water used in all of the experiments and measurements was deionized water with a conductivity of $2.0×10^{-5}$ S/m.

2.2. Flotation tests

Flotation tests were performed on a laboratory XFG_{II} flotation machine with a 35 mL cell (Li and Gao, 2017 and 2018; Tian et al., 2017). In each test, 2.0 g quartz samples and 20 mL water were put into in the flotation cell. After 3 min of stirring, the pH was adjusted to the desired value using NaOH or HCl solutions. Then, after another 3 min of stirring, the activator Ca^{2+} and the collector sodium oleate solutions were added, the conditioning time for each reagent was 3 min. At the end, the flotation lasted for 5 min. The froth products and the tailings were weighed after drying, and the recoveries were calculated based on the weights.

2.3. Adsorption experiments

The adsorption densities of sodium oleate on quartz were measured as a function of pH in the absence and presence of Ca^{2+}. The concentrations of sodium oleate in solutions were determined using an ultraviolet-visible spectrophotometer (UV1901PC, AuCy Instrument, China). The optimal wave length was 230 nm for sodium oleate (Peng et al., 2017). The adsorption amounts were calculated based on the equation:

$$\Gamma = \frac{(C_0 - C)V}{m} \tag{1}$$

where Γ, C_0, C, V, and m was the adsorption density (mol/g), the initial concentration of sodium oleate (mol/L), the sodium oleate concentration after adsorption (mol/L), the volume of the solution (L) and the weight of the sample (g), respectively.

2.4. Zeta potential measurements

A Malvern Nano-ZS90 zeta potential analyzer (Malvern Instruments Ltd. Britain) was used to conduct the zeta potential measurements. In every measurement, 20 mg quartz samples (-5µm) were dispersed into 50 mL KCl ($1×10^{-3}$ mol/L) aqueous solution. After adding certain amounts of reagents, the pH values were regulated by 0.5% HCl or NaOH solutions. Then, the suspension was stirred for 10 min and allowed to settle for 5 min, the supernatant was taken for the measurement.

2.5. DFT calculations

The DFT calculations were performed using the Cambridge serial total energy package (CASTEP) and the DMol3 modules in Accelrys Material Studio 2017 (MS) (Tian et al., 2018). The generalized gradient approximation (GGA) was adopted to accomplish the simulations because of its higher precision than that of the local density approximation (LDA).

The parameter settings, the simulation methods, the property analyses, and the energy calculations were all the same as that reported in the paper of Zhu et al (2016). The computed quartz lattice parameters and the experimental data (Bandura et al., 2011) are listed in Table 1, and the results in Table

428

Physicochem. Probl. Miner. Process., 55(2), 2019, 426-436

1 demonstrated that the simulated quartz crystal was rational enough to represent the real mineral unit cell.

Table 1. The computed and experimental lattice parameters of quartz crystal

Parameters	a=b/Å	c/Å	α=β/°	γ/°
Computed	4.965	5.467	90	120
Experimental	4.914	5.405	90	120
Difference/%	1.04	1.15	0	0

3. Results and discussion

3.1. Effects of pH and Ca^{2+} concentration on the flotation of quartz

The effects of pH on the flotation of quartz in the absence and presence of Ca^{2+} are shown in Fig. 1. Without the help of the activator Ca^{2+}, quartz showed no flotation response to collector sodium oleate over the pH range of 2.1-11.6, the recovery remained at about 0. In the presence of Ca^{2+}, quartz was obviously activated, especially in the strong alkaline region. As the pH increased from 2.1 to 11.5, the flotation recovery of quartz increased from 0 to 98.4%. In the pH range of 11.5-12.0, the recovery kept constant at about 98.4%. The results in Fig. 1 indicated that the activation of Ca^{2+} on quartz mainly took place in the pH range of above 9.5, and the results were in good agreement with previous investigation (Kou et al., 2016).

The effects of Ca^{2+} concentration on the flotation behavior of quartz at pH 11.5 are given in Fig. 2. The recovery of quartz increased from 0 to 98.4% with the Ca^{2+} dosage elevated from 0 to 4×10^{-4} mol/L, and the further increase in the Ca^{2+} concentration caused no noticeable change in the recovery. Thus, with the help of 4×10^{-4} mol/L Ca^{2+} at pH 11.5, the highest recovery of quartz was 98.4% when 2×10^{-3} mol/L sodium oleate was used as the collector.

3.2. Adsorption tests of sodium oleate on quartz surfaces

The adsorption amounts of sodium oleate on quartz surfaces were measured as a function of pH and the concentration of Ca^{2+}, the results are shown in Fig. 3. The initial concentration of sodium oleate in the solution was 2×10^{-3} mol/L.
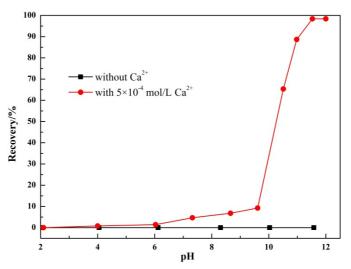

Fig. 1. Flotation recoveries of quartz as a function of pH in the absence and presence of Ca^{2+} using 2×10^{-3} mol/L sodium oleate as the collector

The results in Fig. 3a showed that, in the presence of 4×10^{-4} mol/L Ca^{2+}, the adsorption amounts were very high when pH was lower than 6. However, the recovery of quartz was negligible in the pH range of 2-6. Sodium oleate hydrolyzed to yield oleic acid when pH was below 6 (Peng et al., 2017), and oleic acid was almost insoluble in strong acidic environment. In the adsorption experiments, the

suspensions were centrifuged, and the oily oleic acid could have been adsorbed by the flotation cell surfaces due to its insolubility. Thus, the high adsorption amounts under low pH conditions was not caused by the adsorption of sodium oleate on quartz surfaces. At pH > 8, the adsorption amounts increased with the increasing pH values, and the tendency of the curve in Fig. 3a was in excellent agreement with that of the recovery curve in the presence of Ca^{2+}.
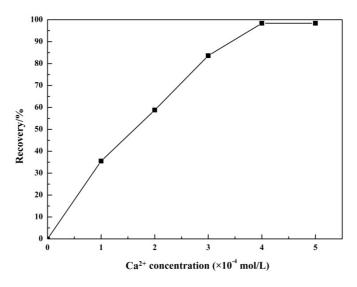

Fig. 2. Effect of Ca^{2+} concentration on the flotation recovery of quartz using 2×10^{-3} mol/L sodium oleate as the collector

The results in Fig. 3b indicated that the increasing in the dosage of Ca^{2+} was favorable to the adsorption of sodium oleate on quartz at pH 11.5. When the concentration of Ca^{2+} was 0, the adsorption amount also was 0, demonstrating that sodium oleate was unable to adsorb on the unactivated quartz surface. The results of the adsorption tests revealed that Ca^{2+} helped the adsorption of sodium oleate on quartz surface, and generated the floatability of quartz, especially under strong alkaline pH conditions.
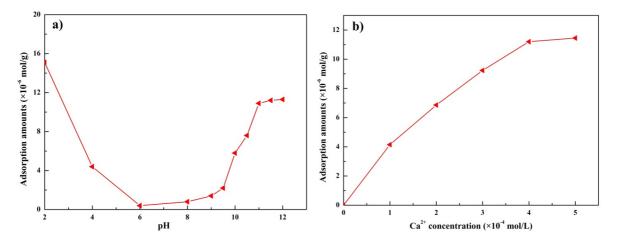

Fig. 3. Adsorption amounts of sodium oleate on quartz surfaces (a) as a function of pH and (b) Ca2+ concentration

3.3. Zeta potential measurements and solution chemistry analyses

The zeta potentials of pure quartz, quartz activated by Ca^{2+}, and quartz conditioned by both Ca^{2+} and sodium oleate were measured, and the results are shown in Fig. 4a. The species distribution diagram of 4×10^{-4} mol/L Ca^{2+} in aqueous solutions are depicted in Fig. 4b. The isoelectric point (IEP) of pure quartz was at 2.1, which was very close to the reported values (Poorni and Natarajan, 2013; Guney et al., 2015; Liu et al., 2017). After being activated by Ca^{2+}, the IEP had no obvious change, but the zeta potentials

shifted significantly towards the positive direction when pH>2. According to the species distribution in Fig. 4b, it was supposed that the adsorption of the positively charged Ca^{2+} or $Ca(OH)^+$ ions on quartz surfaces had caused the positive shift of the potentials (Ozkan et al., 2009; Kou et al., 2016). The Ca^{2+} ions were the dominating species when pH<12.5, but the recovery was extremely low when pH<9.5. When pH exceeded 9.5, the concentration of $Ca(OH)^+$ increased rapidly, the positive shift of the zeta potentials was more remarkable than in lower pH range, and the adsorption amounts of sodium oleate as well as the recovery of quartz also increased rapidly. Moreover, the tendency of the $Ca(OH)^+$ concentration curve was very similar to that of the recovery curve. Besides, the $Ca(OH)_2$ precipitate was generated only when the pH was above 13.1, demonstrating the activation was not attributed to the precipitate. Therefore, it could be inferred that the $Ca(OH)^+$ ion was exactly the functional specie which activated quartz.

The zeta potentials of the quartz that treated both by Ca^{2+} and sodium oleate became more negative than those of the quartz treated only by Ca^{2+}, indicating that the negatively charged oleate anion adsorbed on the activated quartz surfaces (Cao et al., 2013). The negative shift of the zeta potentials was relatively more significant when pH>9.5 than in lower pH range, suggesting more oleate ions had adsorbed on the mineral surfaces, which coincided with the adsorption and flotation tests results. These results underlined why the flotation of quartz occurred under strong alkaline conditions. However, why Ca^{2+} could not activate quartz and how $Ca(OH)^+$ did still remained unexplained. Thus, further investigation was conducted by DFT calculations.
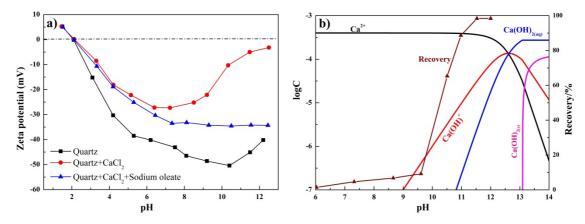

Fig. 4. Zeta potentials of quartz (a), species distribution diagram of Ca^{2+} and flotation recovery of quartz in the presence of Ca^{2+} (b) as a function of pH

3.4. Electronic properties of quartz (101) surface

The (101) surface has been widely recognized as the most favourable quartz cleavage plane responsible for the adsorption of flotation reagents (Rath et al., 2014). The optimized quartz (101) surface slab structure is shown in Fig. 5a, and the Mulliken charge distribution of the surface atoms are listed in Fig. 5b. In Fig. 5, the top layer is displayed in ball-and-stick style and the inner layers are displayed in line style. As it can be seen, at the very top of the quartz (101) surface were the O atoms, and beneath were the "$-O-Si-O-$" frameworks. The negative Mulliken charges in Fig. 5b indicated that the O atoms obtained extra electrons from other atoms, and the positive values suggested that the Si atoms had lost electrons (Zhu et al., 2016). On the quartz (101) surface, the Mulliken charges of the O atoms were in the range from -0.13 to -0.16. The O atoms in the terminal $-Si-O$ dangling bonds held less Mulliken charges than the O atoms bonding with two Si atoms. The Mulliken charges of the Si atoms ranged from 2.19 to 2.37, implying the Si atoms lost electrons.

The density of states (DOS) of the quartz (101) surface are depicted in Fig. 6. A smearing width of 0.1 eV was used to calculate the DOS. The results in Fig. 6 revealed that the 2p orbital of O atoms dominated the peaks near the Fermi level, indicating that the surface O atoms had high reactivity (Gong et al., 2017). According to the Mulliken charge distribution, the quartz (101) surface O atoms had abundant electrons and could donate electrons in chemical interactions. The surface Si atoms almost had no contribution to the Fermi level, and had no extra electrons to offer during adsorption reactions. However, the peaks at

the conduction band derived mainly from the surface Si atoms, implying an ability to accept electrons. The Mulliken charge distribution and DOS of the quartz (101) surface demonstrated that the surface O and Si atoms had the potential to react with the adsorbates.
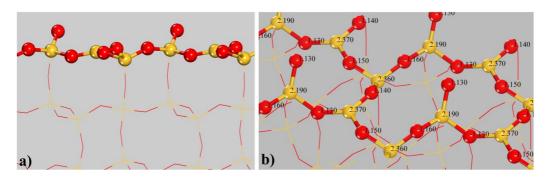

Fig. 5. The quartz (101) surface slab structure (a, side view) and the Mulliken charge distribution of the surface atoms (b, aerial view)
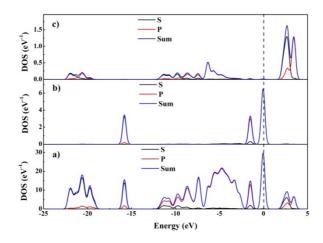

Fig. 6. Density of states of the quartz (101) surface: a) total DOS; b) O atomic DOS; c) Si atomic DOS

3.5. Electronic properties of the adsorbates

The flotation of quartz takes place in strong alkaline aqueous environments, where there are large numbers of OH⁻ ions. These hydroxyl groups greatly influence the surface chemistry of quartz (Zhuravlev, 2000). Therefore, the interaction of OH⁻ with quartz surface is never ignorable. In flotation processes, oleate anion is the functional specie (Rath et al., 2014). In 1952, Fukui Kenichi put forward the FMO theory that the reactivity of a reactant could be reflected by the energy gap between the highest occupied molecular orbital (HOMO) and the lowest unoccupied molecular orbital (LUMO). A narrower energy gap usually indicates a higher chemical reactivity (Tan et al., 2016). Thus, the Mulliken charges and the frontier orbital energy gaps of Ca^{2+}, $Ca(OH)^+$, H_2O, OH⁻ and oleate anion were calculated, the results are listed in Fig. 7 and Table 2.

The Mulliken charge distributions of the adsorbates revealed that the O atoms in $Ca(OH)^+$, H_2O, OH⁻, and oleate anion were all negatively charged, and the Ca atoms in Ca^{2+} and $Ca(OH)^+$ were of positive charges. Hence, O and Ca atoms could be the electron donating or accepting centers, indicating high chemical reactivities (Bag et al., 2011). In addition, the O atoms in H_2O and OH⁻ held more negative charges than the O atoms in oleate anion, which meant stronger electron-donating abilities.

The results in Table 2 suggested that the frontier orbital energy gaps (i.e. E_{LUMO}-E_{HOMO}) followed the order: oleate anion < $Ca(OH)^+$ < OH⁻ < H_2O < Ca^{2+}. Thus, the chemical reactivities of the adsorbates sorted in ascending order as follows: Ca^{2+} < H_2O < OH⁻ < $Ca(OH)^+$ < oleate anion, implying the oleate anion had the maximum potential to react with the quartz surface and the Ca^{2+} had the minimum (Zhao et al., 2013). However, this prediction was not fully in conformity with the flotation results. Therefore, the adsorption of the adsorbates on quartz (101) surface were simulated and discussed.
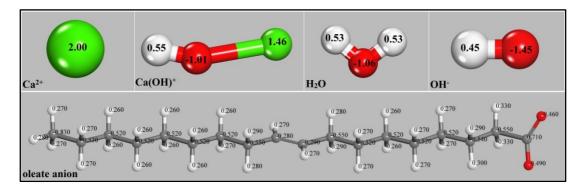
Fig. 7. The Mulliken charge distributions of the adsorbates (colour codes: green=Ca, red=O, white=H, grey=C)

Table 2. The frontier orbital energies of different adsorbates

Adsorbates	Ca^{2+}	$Ca(OH)^+$	H_2O	OH^-	oleate anion
E_{HOMO}/eV	-43.154	-10.905	-6.76	4.824	0.929
E_{LUMO}/eV	-14.462	-7.430	1.048	9.849	1.490
E_{LUMO}-E_{HOMO} /eV	28.692	3.475	7.808	5.025	0.561

3.6. Adsorption of different adsorbates on quartz (101) surface

The optimized adsorbate species were docked on the quartz (101) surface slabs, and the location were determined according to the possible interactions. Dozens of initial adsorption conformations were constructed and optimized, and the most favorable ones were reported. The optimized adsorption configurations of Ca^{2+}, $Ca(OH)^+$, H_2O, OH^-, and oleate anion on quartz (101) surface are shown in Fig. 8, and the corresponding adsorption energies are listed in Table 3. A more negative adsorption energy indicates a stronger adsorption, and a positive adsorption energy means the interaction is unfavorable (Tian et al., 2018; Gao et al., 2018a and b; Guan et al., 2018). Thus, the adsorption energy is a good measure of the adsorption strength (Xu et al., 2016).
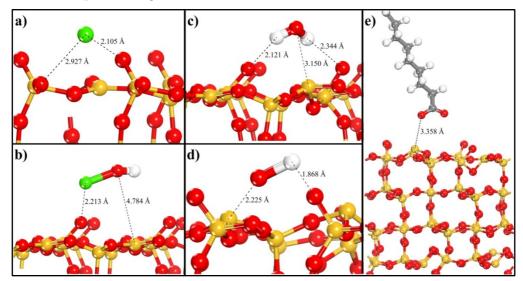

Fig. 8. The optimal adsorption conformations of Ca^{2+} (a), $Ca(OH)^+$ (b), H_2O (c), OH^- (d) and oleate anion (e) on quartz (101) surface (colour codes: green=Ca, red=O, white=H, grey=C, yellow=Si)

The optimization results in Fig. 8 revealed that the Ca^{2+} and $Ca(OH)^+$ were adsorbed on the quartz (101) surface by forming the Ca—O bond. The H_2O molecule was adsorbed through two hydrogen bonds, resulting in the formation of the hydration layer on quartz surface in aqueous solutions (Schlegel et al., 2002). The OH^- ions bonded on the quartz (101) surface through both its O and H atoms, so that the quartz (101) surface was hydroxylated and easily wetted (Miller et al., 2016). However, the O atoms in the $Ca(OH)^+$ and H_2O species were stopped far away from the Si atoms on quartz (101) surface,

indicating no bond was generated. Similar phenomenon happened to the oleate anion, the carboxyl was 0.33 nm away from the nearest Si atom. As it is shown in Fig. 5, each Si atom on quartz (101) surface was surrounded by at least 3 O atoms, and the O atoms were all negatively charged. The sizes of the H_2O, $Ca(OH)^+$ and oleate anion grains were larger than that of the OH^- ion. Thus the H_2O, $Ca(OH)^+$ and oleate anion grains suffered electrostatic repulsion between the O atoms and larger space resistance when approaching the quartz (101) surface, which made it difficult for their O atoms to get close to the surface Si atoms.

Table 3. The adsorption energies of different adsorbates on quartz (101) surface

Adsorbate	Ca^{2+}	$Ca(OH)^+$	H_2O	OH^-	oleate anion
Adsorption energy(kJ/mol)	-15.16	-292.31	-104.87	-206.33	55.61

The interaction energy of oleate anion was 55.61 kJ/mol, this positive value further confirmed that it failed to adsorb on the unactivated quartz (101) surface. The negative adsorption energies of H_2O and OH^-, i. e. -104.87 and -206.33 kJ/mol, demonstrated they adsorbed on the surface spontaneously, resulting in the hydrophilicity of the quartz (101) surface. Flotation takes place in strong alkaline aqueous environments, the quartz particles firstly contact with H_2O and OH^-, thus the water films will easily come into being and make the quartz particles hydrophilic. Without the activation of $Ca(OH)^+$, the oleate anions have no chance to adsorbe on quartz surfaces. The adsorption energy of $Ca(OH)^+$ was -292.31 kJ/mol and much more negative than those of the H_2O and OH^-, implying the adsorption of $Ca(OH)^+$ was more favorable and was able to repulse the hydration film on quartz surface (Liu et al., 2017). That was the reason why $Ca(OH)^+$ activated quartz but Ca^{2+} could not.
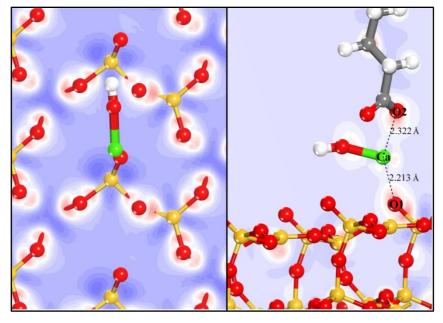

Fig. 9. The $Ca(OH)^+$ activated quartz (101) surface and the adsorption of oleate anion on the activated surface (colour codes: green=Ca, red=O, white=H, grey=C, yellow=Si)

The adsorption of oleate anion on the $Ca(OH)^+$ activated quartz (101) surface was simulated and analyzed subsequently. Here the adsorption of $Ca(OH)^+$ on quartz (101) surface was described as the activating adsorption, and the subsequent adsorption of oleate anion was the collecting adsorption, the results are presented in Fig. 9. The results in Fig. 9 indicated that before the activating adsorption, the quartz (101) surface was dominated by the negatively charged O atoms. The adsorption of $Ca(OH)^+$ provided many island-like activating sites, which decreased the electrostatic repulsion and space resistance between the oleate anion and quartz (101) surface, and facilitated the indirect adsorption of oleate anion on quartz surfaces. The adsorption energy of the collecting adsorption was -339.20 kJ/mol, implying the $Ca(OH)^+$ made the adsorption of oleate anion on quartz surface possible, which was in great agreement with the results of flotation and adsorption tests.

3.7. Electron transfer analyses

The atoms involved in the activating and collecting adsorption were numbered and shown in Fig. 9. The Mulliken charge distributions of the O1, O2, and Ca atoms were calculated to interpret the bond making mechanism during the adsorption processes, and the results are listed in Table 4.

Table 4. The Mulliken charge distributions of the O1, O2 and Ca atoms

Atom	States	s	p	d	Total	Charge/e
O1	Before activating adsorption	1.92	5.21	-	7.13	-1.13
	After activating adsorption	1.89	5.27	-	7.16	-1.16
	After collecting adsorption	1.89	5.26	-	7.15	-1.15
Ca	Before activating adsorption	3.02	5.99	0.44	9.45	0.55
	After activating adsorption	2.17	5.99	0.62	8.78	1.22
	After collecting adsorption	2.12	6.00	0.64	8.76	1.24
O2	Before collecting adsorption	1.84	4.66	-	6.50	-0.49
	After collecting adsorption	1.82	4.88	-	6.70	-0.70

After the activating adsorption, for the Ca atom, the electrons in the 4s orbital decreased from 3.02 to 2.17, and the electrons in the 3d orbital increased from 0.44 to 0.62; for the O1 atom, the electrons in the 2s orbital decreased from 1.92 to 1.89, the electrons in the 2p orbital increased from 5.21 to 5.27. The total electrons of the Ca atom decreased from 9.45 to 8.78, while that of the O1 atom increased from 7.13 to 7.16. It is suggested that when the Ca and O1 atoms got close, their valence electron in s orbitals were excited and jumped to higher energy orbitals. On the whole, the Ca atom lost electrons to the O1 atom. When oleate anion adsorbed on the activated surface, the total electrons of the Ca atom further decreased from 8.78 to 8.76, the total electrons of the O1 atom also decreased from 7.16 to 7.15, and the total electrons of the O2 atom increased from 6.50 to 6.70. Therefore, it was demonstrated that the O1, O2 and Ca atoms were all involved in the collecting adsorption, and electrons transferred via the path of O1$-$Ca$-$O2. The total electrons of the Ca atom decreased after every adsorption. Thus, the Ca(OH)$^+$ acted as an intermediary and electron donor between the quartz (101) surface and oleate anion.

4. Conclusions

Flotation and adsorption tests demonstrated that without the activator Ca^{2+}, quartz showed no flotation behavior, Ca^{2+} greatly promoted the flotation recovery of quartz and the adsorption amounts of sodium oleate on quartz when pH>9.5. Zeta potential measurements and solution chemistry calculations indicated that Ca(OH)$^+$ was exactly the functional specie which activated quartz.

DFT calculations revealed that O atoms dominated the quartz (101) surface, which led to the great electrostatic repulsion and large space resistance between the surface and oleate anions. H$_2$O and OH$^-$ spontaneously adsorbed on the quartz (101) surface and made the surface hydrophilic. Frontier orbital analyses implied that Ca(OH)$^+$ was more chemically active than H$_2$O and OH$^-$; besides, the adsorption energy of Ca(OH)$^+$ on quartz (101) surface was more negative than those of the H$_2$O and OH$^-$, indicating Ca(OH)$^+$ was able to repulse the hydration film on quartz surface. The adsorption of Ca(OH)$^+$ decreased the electrostatic repulsion and space resistance between the oleate anions and quartz (101) surface and facilitated the indirect adsorption of oleate anion on quartz surfaces. Mulliken charge distribution analyses suggested that electrons transition occurred along the path of O1$-$Ca$-$O2, and Ca(OH)$^+$ acted as an intermediary and electron donor in the activation process.

Acknowledgments

References

BAG, B., DAS, B., MISHRA, B. K., 2011. *Geometrical optimization of xanthate collectors with copper ions and their response to flotation.* Miner. Eng. 24, 760-765.

BANDURA, A. V., KUBICKI, J. D., SOFO, J. O., 2011. *Periodic density functional theory study of water adsorption on the a-quartz (101) surface*. J. Phys. Chem. C. 115, 5756-5766.

CAO, Z., ZHANG, Y., CAO, Y., 2013. *Reverse flotation of quartz from magnetite ore with modified sodium oleate*. Min. Proc. Ext. Met. Rev. 34, 320–330.

EL-SALMAWY, M. S., NAKAHIRO, Y., WAKAMATSU, T., 1993. *The role of alkaline earth cations in flotation separation of quartz from feldspar*. Miner. Eng. 6, 1231-1243.

FORNASIERO, D., RALSTON, J., 2005. *Cu(II) and Ni(II) activation in the flotation of quartz,lizardite and chlorite*. Int. J. Miner. Process. 76, 75-81.

FUERSTENAU, M. C., JAMESON, G., YOON, R. H., 2007. *Froth flotation-a century of innovation*. Society of mining, metallurgy, and exploration. Inc 484-486.

GAO, Z.Y., XIE, L., CUI, X., HU, Y.H., SUN, W., ZENG, H.B., 2018a. Probing *Anisotropic Surface Properties and Surface Forces of Fluorite Crystals*. Langmuir 34, 2511-2521.

GAO, Y.S., GAO, Z.Y., SUN, W., YIN, Z.G., WANG, J.J., HU Y.H.,2018b. *Adsorption of a novel reagent scheme on scheelite and calcite causing an effective flotation separation*. J. Colloid Interface Sci. 512, 39-46.

GONG, G. C., HAN, Y. X., LIU, J., ZHU, Y. M., LI, Y. F., YUAN, S., 2017. *In situ investigation of the adsorption of styrene phosphonic acid on cassiterite (110) surface by molecular modeling*. Miner. 7, 181.

GUAN, Q., HU, Y., TANG, H., GAO, Z., SUN, W., 2018. *Preparation of a-CaSO4·½H2O with tunable morphology from flue gas desulphurization gypsum using malic acid as modifier: A theoretical and experimental study*. J. Colloid Interface Sci. 530, 292-301.

GUO, W. D., ZHU, Y. M., HAN, Y. X., WEI, Y. H., 2018. *Effects and activation mechanism of calcium ion on the flotation of quartz with fatty acid collector*. J. Northeast. Univ. 39, 409-415. (in Chinese)

GUNEY, A., ÖZDILEK, C., KANGAL, M.O., BURAT, F., 2015. *Flotation characterization of PET and PVC in the presence of different plasticizers*. Sep. Purif. Technol. 151, 47–56.

JIN, J. X., GAO, H. M., CHEN, X. M., PENG, Y. J., 2016. *The separation of kyanite from quartz by flotation at acidic pH*. Miner. Eng. 92, 221-228.

KOU, J., XU, S., SUN, T., SUN, C., GUO, Y., WANG, C., 2016. *A study of sodium oleate adsorption on Ca^{2+} activated quartz surface using quartz crystal microbalance with dissipation*. Int. J. Miner. Process. 154, 24-34.

LI, C., GAO Z., 2018. *Tune surface physicochemical property of fluorite particles by regulating the exposure degree of crystal surfaces*. Miner. Eng. 128, 123-132.

LI, C., GAO Z., 2017. *Effect of grinding media on the surface property and flotation behavior of scheelite particles*. Powder Technol. 322, 386-392.

LIU, J., GONG, G. C., HAN, Y. X., ZHU, Y. M., 2017. *New insights into the adsorption of oleate on cassiterite: A DFT study*. Miner. 7, 236.

LIU, W. B., LIU, W. G., WEI, D. Z., LI, M. Y., ZHAO, Q., XU, S. C., 2017. *Synthesis of N,N-Bis(2-hydroxypropyl)laurylamine and its flotation on quartz*. Chem. Eng. J. 309, 63-69.

LUO, X. M., WANG, Y. F., WEN, S. M., MA, M. Z., SUN, C. Y., YIN, W. Z., MA, Y. Q., 2016. *Effect of carbonate minerals on quartz flotation behavior underconditions of reverse anionic flotation of iron ores*. Int. J. Miner. Process. 152, 1-6.

MILLER, J. D., WANG, X., JIN, J., SHRIMALI, K., 2016. *Interfacial water structure and the wetting of mineral surfaces*. Int. J. Miner. Process. 156, 62-68.

OZKAN, A., UCBEYIAY, H., DUZYOL, S., 2009. *Comparison of stages in oil agglomeration process of quartz with sodium oleate in the presence of Ca(II) and Mg(II) ions*. J. Colloid. Interf. Sci. 329, 81-88.

PENG, H. Q., LUO, W., WU, D., BIE, X. X., SHAO, H., JIAO, W. Y., LIU, Y. K., 2017. *Study on the effect of Fe^{3+} on zircon flotation separation from cassiterite using sodium oleate as   collector*. Miner. 7, 108.

POORNI, S., NATARAJAN, K.A., 2013. *Microbially induced selective flocculation of hematite from kaolinite*. Int. J. Miner. Process. 125, 92–100.

RATH, S. S., SAHOO, H., DAS, B., MISHRA, B. K., 2014. *Density functional calculations of amines on the (1 0 1) face of quartz*. Miner. Eng. 69, 57-64.

RATH, S.S., SINHA, N., SAHOO, H., DAS, B., MISHRA, B.K., 2014. *Molecular modeling studies of oleate adsorption on iron oxides*. Appl. Surf. Sci. 295, 115-122.

SCHLEGEL, M.L., NAGY, K.L., FENTER, P., STURCHIO, N.C., 2002. *Atomic-scale structure of the quartz (10(1)over-bar-0)- and (10(1)over-bar-1)-water interfaces*. Geochim. Cosmochim. Ac. 66, A679-A679.

TAN, X., HE, F. Y., SHANG, Y. B., YIN, W. Z., 2016. *Flotation behavior and adsorption mechanism of (1-hydroxy-2-*

methyl-2-octenyl) phosphonic acid to cassiterite. Trans. Nonferrous Met. Soc. China. 26, 2469-2478.

TIAN, M., GAO, Z., SUN, W., HAN, H., SUN, L., HU, Y., 2018. *Activation role of lead ions in benzohydroxamic acid flotation of oxide minerals: New perspective and new practice.* J. Colloid Interface Sci. 529, 150-160.

TIAN, M., GAO, Z., HAN, H., SUN, W., HU, Y., 2017. Improved flotation separation of cassiterite from calcite using a mixture of lead (II) ion / benzohydroxamic acid as collector and carboxymethyl cellulose as depressant. Miner. Eng. 113, 68-70.

WANG, D. Z., 1988. *Chemistry of flotation solutions.* Hunan Science and Technology Press, Changsha, P. 138.

XU, L. H., HU, Y. H., Wu, H. Q., Tian, J., Liu, J., Gao, Z. Y, WANG, L., 2016. *Surface crystal chemistry of spodumene with different size fractions and implications for flotation.* Sep. Purif. Technol. 169, 33-42.

YE, H., MATSUOKA, I., 1993. *Reverse flotation of fine quartz from dickite with oleate.* Int. J. Miner. Process. 40, 123-136.

YIN, W. Z., LI, D., LUO, X. M., YAO, J., SUN, Q. Y., 2016. *Effect and mechanism of siderite on reverse flotation of hematite.* Int. J. Min. Met. Mater. 23, 373-379.

ZHANG, J., WANG, W. Q., LIU, J., HUANG, Y., FENG, Q. M., ZHAO, H., 2014. *Fe(III) as an activator for the flotation of spodumene, albite, and quartz minerals.* Miner. Eng. 61, 16-22.

ZHAO, G., ZHONG, H., QIU, X. Y., WANG, S., GAO, Y. D., DAI, Z. L., HUANG, J., LIU, G. Y., 2013. *The DFT study of cyclohexyl hydroxamic acid as a collector in scheelite flotation.* Miner. Eng. 49, 54-60.

ZHU, Y. M., LUO, B. B., SUN, C. Y., LIU, J., SUN, H. T., LI, Y. J., HAN, Y. X., 2016. *Density functional theory study of a-Bromolauric acid adsorption on the a-quartz (101) surface.* Miner. Eng. 92, 72-77.

ZHURVALEV, L. T., 2000. *The surface chemistry of amorphous silica. zhuravlev model.* Colloid. Surface. A. 173, 1-38.